Equatorial and related non-equilibrium states in magnetization dynamics of ferromagnets: Generalization of Suhl's spin-wave instabilities

C. Kosaka [a], K. Nakamura [a], S. Murugesh [b], M. Lakshmanan [b],*

[a]*Department of Applied Physics, Osaka City University, Osaka 558-8585, Japan*

[b]*Centre for Nonlinear Dynamics, Department of Physics, Bharathidasan University, Tiruchirappalli 620024, India*

Abstract

We investigate the nonlinear dynamics underlying the evolution of a 2-D nanoscale ferromagnetic film with uniaxial anisotropy in the presence of perpendicular pumping. Considering the associated Landau-Lifshitz spin evolution equation with Gilbert damping together with Maxwell equation for the demagnetization field, we study the dynamics in terms of the stereographic variable. We identify several new fixed points for suitable choice of external field in a rotating frame of reference. In particular, we identify explicit equatorial and related fixed points of the spin vector in the plane transverse to the anisotropy axis when the pumping frequency coincides with the amplitude of the static parallel field. We then study the linear stability of these novel fixed points under homogeneous and spin wave perturbations and obtain a generalized Suhl's instability criterion, giving the condition for exponential growth of P-modes under spin wave perturbations. Two parameter phase diagrams (in terms of amplitudes of static parallel and oscillatory perpendicular magnetic fields) for stability are obtained, which differ qualitatively from those for the conventional ferromagnetic resonance near thermal equilibrium and are amenable to experimental tests.

Key words: Nonlinear spin dynamics, Landau-Lifshitz equation, Magnetic resonance, Suhl instability
PACS: 67.75.Lm, 76.50.+g, 75.10.Hk

---

* Corresponding author.
  Email address: `lakshman@cnld.bdu.ac.in` (M. Lakshmanan).

1 Introduction

Interest in ferromagnetic resonance (FMR) has soared in recent times due to advances in fabricating nanostructures. This implies prospects for several new experiments to study possible absorption phenomena, and patterns that may form owing to instabilities, in ferromagnetic films. While other magnetic resonance counterparts such as nuclear magnetic resonance(NMR), electron paramagnetic resonance(EPR), electron spin resonance, etc., have found immense technological applications, including crystal structure determination and medical diagnostics, FMR has remained a more complex phenomenon. Some of the main features of FMR are a) large magnetization, and hence large susceptibility, b) large demagnetization field due to strong magnetization, which is also influenced by the shape of the specimen, and c) resonance excitations breaking into spin wave modes, that make spin reversal more complex.

Spin-wave instabilities were first observed independently by Damon [1] and by Bloembergen and Wang [2] as noisy anomalous absorption which abruptly sets in at a certain threshold power as the resonant microwave field is increased. Suhl remarked that this phenomenon "bears a certain resemblance to the turbulent state in fluid mechanics" [3] . In fact the instabilities in this case were first explored in [3] and are referred to as *Suhl instability*. These were subsequently verified experimentally [4].

Under a growing attention to deterministic chaos and nonlinear dynamics, there occurred a renaissance on studies involving high-power magnetic resonance in the 1980s. High-resolution experiments were carried out for spin-wave nonlinear dynamics in the yttrium iron garnet film and sphere in parallel and perpendicular pumpings [5,6,7,8]. For certain high powers beyond the Suhl threshold, interaction between excited spin-wave modes lead to various dynamical phenomena including auto-oscillations, period-doubling cascades, quasi-periodicity, and chaos. Also observed were irregular relaxation oscillations and abrupt transitions to wide-band turbulence, beyond the Suhl threshold [5,6,7,8], which were explained by using Zakharov et al's *S-theory* [9]. Since then the studies on spin wave instabilities have acquired renewed interests up to now [10,11,12].

Despite these pioneering works, including that of Suhl[3], the investigations have been limited to the instability around fixed points that correspond to magnetization parallel to the anisotropy axis. This is due to the following fact: In contrast to the case of NMR and EPR, macroscopic ferromagnets in FMR have large frozen magnetization. Under a static magnetic field, therefore, any available pumping field cannot freely rotate such strong magnetization at the cost of the large stabilizing energy (Zeeman energy). In nanoscale ferromagnets, however, it is possible to rotate the saturation magnetization far from

2

the anisotropy axis. The magnetization can even be driven to the equatorial plane perpendicular to the anisotropy axis. Therefore it is timely to analyze the nonlinear dynamics of spin waves in these new non-equilibrium states.

It may also be noted that a number of investigations exist in the literature on the dynamics of higher dimensional Heisenberg ferromagnetic spin systems [13,14,15] corresponding to isotropic (pure exchange interaction), anisotropic, external field and other interactions [13,14,15,16,17]. However, to the knowledge of the authors, concerning the systems coupled with Maxwell equation for the demagnetization field as considered as in this paper, there exist very few studies.

In this article, we investigate a 2-D ferromagnetic system with uniaxial anisotropy in a background of alternating magnetic field transverse to, and a static magnetic field parallel to, the anisotropy axis. The axis of anisotropy is chosen to be arbitrary. We also include the demagnetization field due to the spatial inhomogeneity of the magnetization vector, which is seen to play a crucial role. Fixed points - P-modes - of such a system have been identified earlier, and their stability against both homogeneous perturbations and spin-wave excitations analyzed [18,19]. However, we specifically analyze equatorial and other fixed points, that have not been identified earlier, wherein the average magnetization vector lies in the plane transverse to the anisotropy axis and exhibit a more complex dynamics. We further obtain a criterion for instability under spin wave excitations, thus generalizing the Suhl's instability criterion.

The strategy we follow in our analysis is as follows. We project the unit spin vector $\hat{\mathbf{m}}(\mathbf{r}, t)$ stereographically onto a complex plane $\psi(\mathbf{r}, t)$ and deduce the equation of motion in terms of the stereographic variable. Now going over to a natural rotating frame of reference, one is able to identify the defining equations for the fixed points or the so called P-modes. Of all the possible equilibrium points, the equatorial and related fixed points are of special interest as their expressions can be explicitly obtained. In fact we find that there exists four such equilibrium points. Then we investigate their linear stability nature (i) under spatially homogeneous perturbations and (ii) under more general spin wave perturbation in order to identify their local and global stability, and obtain conditions for Suhl's instability as a function of experimentally measurable parameters such as the amplitudes of oscillatory perpendicular and static parallel external magnetic fields. The results give clear criteria for experimental realization of the predicted results.

The plan of the paper is as follows. In Section 2, we introduce the model spin Hamiltonian for the ferromagnetic film in the presence of the external field and an intrinsic demagnetization field, and write down the Landau-Lifshitz (LL) equation for the spin field with the Gilbert damping term included. We further introduce the stereographic variable, and rewrite the LL equation in terms of

the new variable. In Section 3, we identify fixed points of the LL equation, specifically the equatorial and other related fixed points, and analyze their linear stability under homogeneous perturbations. In Section 4, we study the stability of these fixed points under spin wave excitations in terms of a period map and generalize Suhl's instability criterion. We conclude with a summary of results in Section 5.

2 Model Hamiltonian and LL equation

We consider a 2-D ferromagnetic film with uniaxial anisotropy and an applied oscillating magnetic field in the direction transverse to the anisotropy axis. Such a system can be described by a Hamiltonian for the unit spin field $\hat{\mathbf{m}}(\mathbf{r}, t) = \{m_1(\mathbf{r}, t), m_2(\mathbf{r}, t), m_3(\mathbf{r}, t)\}; \quad \hat{\mathbf{m}}^2 = 1$ as

$$H = H_{exchange} + H_{applied} + H_{anisotropy} + H_{demagnetization}, \tag{1}$$

where

$$H_{exchange} = \int D(\nabla \hat{\mathbf{m}})^2 \, d^2\mathbf{r}, \tag{2}$$

$$H_{applied} = -\int \mathbf{B}_a \cdot \hat{\mathbf{m}} \, d^2\mathbf{r}, \tag{3}$$

$$H_{anisotropy} = -\int \kappa m_{\parallel}^2 \, d^2\mathbf{r}, \tag{4}$$

$$H_{demagnetization} = -\int \mathbf{H}_m \cdot \hat{\mathbf{m}} \, d^2\mathbf{r}, \tag{5}$$

and the demagnetizing field $\mathbf{H}_m$ satisfies the Maxwell's equation,

$$\nabla \cdot \mathbf{H}_m = -4\pi \nabla \cdot \hat{\mathbf{m}}; \quad \nabla \times \mathbf{H}_m = 0. \tag{6}$$

In the above, we have assumed the average magnetization to be of constant magnitude in space and time, and hence conveniently expressed the Hamiltonian (1) in terms of the normalized unit average magnetization $\hat{\mathbf{m}}$. Equation (6) gives the constitutive relation connecting the demagnetization field with the average local magnetization, assuming absence of any free current in the film. In equations (2-5), D is the exchange constant, $\mathbf{B}_a$ is the applied magnetic field, κ is the anisotropy parameter and $m_{\parallel}$ is the component of magnetization in the direction of anisotropy.

4

Time evolution of the spin field is governed by the Hamilton's equation

$$\dot{\mathbf{m}} = \frac{\delta H}{\delta \hat{\mathbf{m}}} = \{\hat{\mathbf{m}}, H\}. \tag{7}$$

Using the spin Poisson bracket relations

$$\{m_i(\mathbf{r}, t), m_j(\mathbf{r}', t')\} = \epsilon_{ijk} m_k \delta(\mathbf{r} - \mathbf{r}', t - t'), \tag{8}$$

it is straight forward to show that the dynamics is governed by the LL equation[20],

$$\dot{\hat{\mathbf{m}}} = -\hat{\mathbf{m}} \times \mathbf{F}_{eff}, \tag{9}$$

where $\mathbf{F}_{eff}$ is the effective field given by

$$\mathbf{F}_{eff} = D\nabla^2 \hat{\mathbf{m}} + \mathbf{B}_a + \kappa m_{\parallel} \hat{e}_{\parallel} + \mathbf{H}_m. \tag{10}$$

In equation (10), ∇^2 is the two dimensional Laplacian $\nabla^2 = \partial^2/\partial x^2 + \partial^2/\partial y^2$. The direction of anisotropy $\hat{e}_{\parallel}$ has been chosen to be arbitrary in the internal space of the spin field. Further, writing $\hat{e}_{\parallel} = \{0, 0, 1\}$, we choose the applied magnetic field to be of the form

$$\mathbf{B}_a = h_{a\perp}\{\cos\omega t, \sin\omega t, 0\} + h_{a\parallel}\hat{e}_{\parallel} \equiv h_{a\perp}(\cos\omega t \hat{e}_1 + \sin\omega t \hat{e}_2) + h_{a\parallel}\hat{e}_{\parallel}, \tag{11}$$

where $\hat{e}_1$ and $\hat{e}_2$ are two unit orthonormal vectors in the plane transverse to the anisotropy axis. Notice that the orientation of the anisotropy axis is specified as in equation (11) in the spin space, but is still arbitrary in the physical space, where the plane of the ferromagnetic film is assumed to be in the $x - y$ direction. Without loss of generality one can choose $m_{\parallel} = m_3$. Introducing a phenomenological Gilbert damping term (proportional to α), equation (9) can be modified to the form

$$\dot{\hat{\mathbf{m}}} - \alpha\hat{\mathbf{m}} \times \dot{\hat{\mathbf{m}}} = -\hat{\mathbf{m}} \times \mathbf{F}_{eff}. \tag{12}$$

It is this equation in 2-D coupled with the Maxwell equation which we shall investigate in this paper.

It proves convenient for later analysis to express the equation in terms of the complex stereographic variable (see Figure 1 for details)

$$\psi \equiv \frac{m_1 + im_2}{1 + m_3}, \tag{13}$$

or equivalently by the transformation

$$\hat{\mathbf{m}} = \frac{1}{1 + |\psi|^2}\{2Re\psi, 2Im\psi, 1 - |\psi|^2\}. \tag{14}$$

Correspondingly, the terms in the Hamiltonian in equation (1) become

$$H_{exchange} = \int D\frac{|\nabla\psi|^2}{(1 + |\psi|^2)^2} \, d^2\mathbf{r}, \tag{15}$$

$$H_{applied} = -\int \Big[h_{a\perp}\frac{\psi e^{-i\omega t} + \psi^* e^{i\omega t}}{1 + |\psi|^2} + h_{a\parallel}\frac{(1 - |\psi|^2)}{(1 + |\psi|^2)}\Big] \, d^2\mathbf{r}, \tag{16}$$

$$H_{anisotropy} = -\int \kappa\frac{(1 - |\psi|^2)^2}{(1 + |\psi|^2)^2} \, d^2\mathbf{r}, \tag{17}$$

$$H_{demagnetization} = -\int \Big[\frac{H_m^*\psi + H_m\psi^*}{1 + |\psi|^2} + h_{m\parallel}\frac{(1 - |\psi|^2)}{(1 + |\psi|^2)}\Big] \, d^2\mathbf{r}, \tag{18}$$

where we have used equation (11), and represented the demagnetization field as $\mathbf{H}_m = \{h_1, h_2, h_{m\parallel}\}$ with $H_m = h_1 + ih_2$.

On account of the spin Poisson bracket relations in equation (8), ψ obeys the Poisson bracket relation,

$$\{\psi(\mathbf{r}, t), \psi^*(\mathbf{r}', t')\} = i\delta(\mathbf{r} - \mathbf{r}', t - t'). \tag{19}$$

For the complex scalar field ψ, one can write down the evolution equation from the Hamiltonian (1), equivalent to equation (9). Then, including the damping term, the evolution equation for ψ equivalent to equation (12) reads as [21]

$$i(1 - i\alpha)\dot{\psi} = D(\nabla^2\psi - 2\frac{\psi^*(\nabla\psi)^2}{1 + |\psi|^2}) - (h_{a\parallel} + \kappa\frac{1 - |\psi|^2}{1 + |\psi|^2})\psi \tag{20}$$

$$+\frac{1}{2}h_{a\perp}(e^{i\omega t} - \psi^2 e^{-i\omega t})$$

$$-h_{m\parallel}\psi + \frac{1}{2}(H_m - \psi^2 H_m^*).$$

The form of the applied transverse field in equation (20) suggests that it is convenient to make a transformation

$$\psi = \hat{\psi}(\mathbf{r}, t)\exp[i\omega t], \tag{21}$$

and rewrite equation (20) in terms of $\hat{\psi}$. This amounts to moving to a rotating coordinate frame in the spin space, rotating about the anisotropy axis $\hat{e}_\parallel$ with angular frequency ω. If $\hat{\mathbf{m}}$ were expressed in spherical polar coordinates in the rotating frame as $\hat{\mathbf{m}} = \{\sin\theta\cos\phi, \sin\theta\sin\phi, \cos\theta\}$, then $\hat{\psi} = \tan(\theta/2)\exp i\phi$. With this change, the equation (20) becomes

$$i(1 - i\alpha)\dot{\hat{\psi}} = D(\nabla^2\hat{\psi} - 2\frac{\hat{\psi}^*(\nabla\hat{\psi})^2}{1 + |\hat{\psi}|^2}) - (h_{a\parallel} - \omega + i\alpha\omega + \kappa\frac{1 - |\hat{\psi}|^2}{1 + |\hat{\psi}|^2})\hat{\psi} \quad (22)$$
$$+ \frac{1}{2}h_{a\perp}(1 - \hat{\psi}^2)$$
$$- h_{m\parallel}\hat{\psi} + \frac{1}{2}(H_m e^{-i\omega t} - \hat{\psi}^2 H_m^* e^{i\omega t}).$$

It must be remembered that $h_{m\parallel}$, H_m and H_m^* in equation (22) are intrinsically related to $\hat{\psi}$ through the relation (6). Due to the second equation in (6), we can write

$$\mathbf{H}_m = -\nabla\varphi, \tag{23}$$

by introducing an auxiliary potential $\varphi(\mathbf{r}, t)$. Thus, $\mathbf{H}_m$ can be found by solving the Poisson equation $\nabla^2\varphi = -4\pi\nabla\cdot\hat{\mathbf{m}}$. Consequently, the boundary condition and shape of the boundary influence the actual form of φ, and hence $\mathbf{H}_m$. In the following we shall consider only spatially homogeneous spin fields and small amplitude spin waves. In this case, boundary effects can be ignored if one assumes the spin wave to be confined to a localized region, and that they dissipate close to the boundary. In the case of large amplitude perturbations, coupling between different modes become nontrivial. This case will be separately treated elsewhere.

3   Fixed points (P-modes) and stability

Spatially homogeneous fixed points of equation (22) correspond to a uniform magnetization field that exhibit a periodic motion of frequency ω, irrespective of the fact that the governing equations are highly nonlinear. Such homogeneous steady states in the rotating frame are referred to as P-modes. These fixed points $\hat{\psi}_o$, in the moving frame, are obtained from equation (22) by assuming time independence and spatial homogeneity of $\hat{\psi}$, i.e., $\partial\hat{\psi}_o/\partial t = 0 = \nabla\hat{\psi}_o$. For such a uniform steady field $\hat{\psi}_o$, the uniform demagnetization field can be conveniently written as $\mathbf{H}_m^o = -N_\perp\mathbf{m}_\perp^o - N_\parallel\mathbf{m}_\parallel^o$, where $\mathbf{m}_\perp^o = \{m_1^o, m_2^o, 0\}$,

i.e.,

$$H_m^o = -N_\perp(m_1^o + im_2^o) = -2\frac{N_\perp \hat{\psi}_o}{1 + |\hat{\psi}_o|^2}e^{i\omega t}; \tag{24}$$

$$h_{m\parallel} = -N_\parallel m_\parallel^o = -N_\parallel \frac{1 - |\hat{\psi}_o|^2}{1 + |\hat{\psi}_o|^2}. \tag{25}$$

Using these conditions in equation (22), one obtains after some rearrangement, the equation for the fixed points as

$$(b_{a\parallel} + i\Omega + \frac{1 - |\hat{\psi}_o|^2}{1 + |\hat{\psi}_o|^2})\hat{\psi}_o - \frac{1}{2}b_{a\perp}(1 - \hat{\psi}_o^2) = 0, \tag{26}$$

where the quantities $b_{a\parallel}, b_{a\perp}, \Omega$ and κ_{eff} are defined as

$$b_{a\parallel} = \frac{h_{a\parallel} - \omega}{\kappa_{eff}}; \quad b_{a\perp} = \frac{h_{a\perp}}{\kappa_{eff}}; \quad \Omega = \frac{\alpha\omega}{\kappa_{eff}}; \quad \kappa_{eff} = \kappa + N_\perp - N_\parallel. \tag{27}$$

Evidently, the fixed points are functions of the applied field strengths $h_{a\perp}$ and $h_\parallel$, and the frequency ω, besides the anisotropy constant κ. However, of these $h_\parallel, h_{a\perp}$ and ω are the tunable parameters.

From equation (26), it is straightforward to check that the equation satisfied by $|\hat{\psi}_o|^2$ is,

$$|\hat{\psi}_o|^2\Big(b_{a\parallel} + \frac{1 - |\hat{\psi}_o|^2}{1 + |\hat{\psi}_o|^2}\Big)^2 + \Omega^2|\hat{\psi}_o|^2\Big(\frac{1 - |\hat{\psi}_o|^2}{1 + |\hat{\psi}_o|^2}\Big)^2 = \frac{b_{a\perp}^2}{4}(1 - |\hat{\psi}_o|^2)^2. \tag{28}$$

Equation (28) can be rewritten as a polynomial of degree four in $u = |\hat{\psi}_o|^2$ as

$$-\frac{b_{a\perp}^2}{4}u^4 + (b_{a\parallel}^2 - 2b_{a\parallel} + 1 + \Omega^2)u^3 + (2b_{a\parallel}^2 - 2 - 2\Omega^2 + \frac{b_{a\perp}^2}{2})u^2 \tag{29}$$
$$+(b_{a\parallel}^2 + \Omega^2 + 1 + 2b_{a\parallel})u - \frac{b_{a\perp}^2}{4} = 0.$$

The quartic equation (29) admits in general zero, two or four real solutions depending on the sign and magnitude of the coefficients. These roots can be easily obtained for any given set of parameters, and the nature of the corresponding fixed points can be analyzed by means of standard theory of equilibrium points of two-dimensional dynamical systems. One can establish the presence of either stable modes or foci, unstable nodes or foci, or saddles.

A detailed analysis of these modes in terms of polar coordinates has been made in the past by Bertotti et. al. [18].

In this paper, we wish to concentrate on certain physically interesting modes not identified earlier, namely those arising out of fixed points along the equator or related fixed points, whose form can be explicitly determined. Consequently their stability analysis can also be carried out in detail. In particular, on account of the anisotropy, the tendency for the spin field is to orient along the direction of $\pm \hat{e}_{\parallel}$. Naturally, the fixed points along the equator, i.e., in the $\hat{e}_1 - \hat{e}_2$ plane, are special, being the other extreme, but are available in nonequilibrium nano-ferromagnets. Besides, as will be shown below, these fixed points are degenerate, and the nature of dynamics around these fixed points is naturally of considerable interest. In the next three sections, we identify these fixed points and study their stability under homogeneous and spin wave perturbations. In Section 4.2, we obtain the generalization of the Suhl's instability criterion.

3.1 Equatorial and related fixed points

In this section we identify fixed points along the equator and others related to them, and analyze their stability under homogeneous perturbations.

Along the equator, we have $m_{\parallel}^o(= m_3^o) = 0$, or $|\hat{\psi}_o|^2 = 1$. Conversely, $|\hat{\psi}_o|^2 = 1$ implies spins are pointed in the equatorial plane. But from equation (28),fixed points along the equator are possible only when $b_{a\parallel} = 0$,or $h_{a\parallel} = \omega$. However for this choice of the pumping frequency ω or the equivalent amplitude of the static parallel field $h_{a\parallel}$, other related fixed points also exist. In fact with this choice, equation (26) can be solved to obtain four fixed points P_1, P_2, P_3 and P_4:

$$\frac{\hat{\psi}_{oIm}}{\hat{\psi}_{oRe}} = \tan\phi = -\Omega; \tag{30}$$

$$P_1 = P_2 : |\hat{\psi}_o|^2 = 1; \tag{31}$$

$$P_3 : |\hat{\psi}_o|^2 = \frac{2(1+\Omega^2)}{b_{a\perp}^2}\left[1 + \sqrt{1 - \frac{b_{a\perp}^2}{1+\Omega^2}}\right] - 1; \tag{32}$$

$$P_4 : |\hat{\psi}_o|^2 = \frac{2(1+\Omega^2)}{b_{a\perp}^2}\left[1 - \sqrt{1 - \frac{b_{a\perp}^2}{1+\Omega^2}}\right] - 1. \tag{33}$$

The fixed points are adjusted by tuning the transverse field strength $h_{a\perp}(= \kappa_{eff}b_{a\perp})$ and the frequency $\omega(= \kappa_{eff}\Omega/\alpha)$ of the applied field, while keeping $h_{a\parallel} = \omega$. Equations (31)-(33) also impose a limit on the applied transverse

9

field strength, namely, $0 \leq b_{a\perp}^2 \leq 1 + \Omega^2$. In terms of the original variables this condition becomes $0 \leq h_{a\perp}^2 \leq \kappa_{eff}^2 + \alpha^2\omega^2$.

From equation (28) we notice that there are four solutions to $|\hat{\psi}_o|^2$ as seen above. Of these four, two fixed points, (P_1, P_2) merge $(|\hat{\psi}_o|^2 = 1)$ with the choice $b_{a\|} = 0$, or $h_{a\|} = \omega$. These fixed points lie along the equator, transverse to $\hat{e}_\|$. The other two related fixed points (P_3, P_4) in equations (31-33) vary between south pole $(|\hat{\psi}_o|^2 = \infty)$ and equator for the range $0 \leq b_{a\perp}^2 \leq 1 + \Omega^2$. The exact orientation will also be decided by the azimuthal angle ϕ determined by Ω, as in equation (30). Particularly, for the choice $b_{a\perp}^2 = 1 + \Omega^2$, i.e., $h_{a\perp}^2 = \kappa_{eff}^2 + \alpha^2\omega^2$, the only possible fixed points are along the equator.

3.2 Spatially homogeneous perturbations

For a spatially homogeneous perturbation $\delta\hat{\psi}(t)$ from $\hat{\psi}_o$, the linear stability of $\hat{\psi}_o$ is analyzed using equation (22), with the assumption $\hat{\psi} = \hat{\psi}_o + \epsilon\delta\hat{\psi}, \epsilon << 1$, and restricting to linear terms in $\delta\hat{\psi}$. Correspondingly, the perturbed equation reads as

$$i(1 - i\alpha)\delta\dot{\psi} = -\kappa_{eff}(i\Omega + \frac{1 - |\hat{\psi}_o|^2}{1 + |\hat{\psi}_o|^2})\delta\hat{\psi} + 2\kappa_{eff}\Gamma\hat{\psi}_o(\hat{\psi}_o\delta\hat{\psi}^* + \hat{\psi}_o^*\delta\hat{\psi}) \quad (34)$$
$$-h_{a\perp}\hat{\psi}_o\delta\hat{\psi},$$

where we have defined $\Gamma = (1 + |\hat{\psi}_o|^2)^{-2}$. The equation (34) and its complex conjugate can be written in a compact form using an appropriate matrix $\mathbf{\Lambda}$, as

$$\frac{d\Psi}{dt} = \Lambda \cdot \Psi, \tag{35}$$

with

$$\mathbf{\Lambda} = \begin{pmatrix} \frac{i\kappa_{eff}}{1-i\alpha}\left[i\Omega + \frac{1-|\hat{\psi}_o|^2}{1+|\hat{\psi}_o|^2} - 2\Gamma|\hat{\psi}_o|^2 \right. & \frac{-2i\kappa_{eff}}{1-i\alpha}\Gamma\hat{\psi}_o^2 \\ \left. +b_{a\perp}\hat{\psi}_o\right] & \\ & \frac{-i\kappa_{eff}}{1+i\alpha}\left[-i\Omega + \frac{1-|\hat{\psi}_o|^2}{1+|\hat{\psi}_o|^2} - 2\Gamma|\hat{\psi}_o|^2 \right. \\ \frac{2i\kappa_{eff}}{1+i\alpha}\Gamma\hat{\psi}_o^{*2} & \left. +b_{a\perp}\hat{\psi}_o^*\right] \end{pmatrix} \quad (36)$$

and $\Psi = (\delta\hat{\psi}, \delta\hat{\psi}^*)^T$. The type of instability of a fixed point is determined by the determinant and trace of $\mathbf{\Lambda}$. Defining $\chi = (1 - |\hat{\psi}_o|^2)/(1 + |\hat{\psi}_o|^2)$, from

equation (34), the determinant and trace are found to be

$$|\mathbf{\Lambda}| = \frac{\kappa_{eff}}{1+\alpha^2}\chi^2(1+\Omega^2),$$ (37)

$$Tr(\mathbf{\Lambda}) = -2\alpha\frac{\kappa_{eff}}{1+\alpha^2}(\frac{1+\chi^2}{2}+\frac{\chi\Omega}{\alpha}).$$ (38)

In general, the fixed point is a stable node or foci if $|\mathbf{\Lambda}| > 0$ and $Tr\mathbf{\Lambda} < 0$, an unstable node or foci in case $|\mathbf{\Lambda}| > 0$ and $Tr\mathbf{\Lambda} > 0$, and a saddle if $|\mathbf{\Lambda}| < 0$. However, for the equatorial fixed points $|\hat{\psi}_o|^2 = 1$, and consequently $|\mathbf{\Lambda}| = 0$, since $\chi = 0$, thus leading to degeneracy. In order to identify the nature of these fixed points, we directly solve equation (22) numerically in the neighborhood of the fixed points, assuming spatial inhomogeneity of $\hat{\psi}$ and plot the resultant phase portrait in Figure 2. Figure 2(a) shows the phase portrait for the choice $b_{a\perp}^2 = 1+\Omega^2$, for which the only fixed points are along the equator (P_1andP_2), as remarked earlier. Figure 2(b) is for the choice $b_{a\perp}^2 = (1+\Omega^2)/2$, for which there are two additional fixed points at $\hat{\psi}_o = (2.4, -0.2)(P_3)$ and $\hat{\psi}_o = (0.41, -0.03)(P_4)$.

4   Equatorial and related fixed points and spin-wave instability

Unlike in EPR and NMR, spin reversal is prevented in ferromagnetic resonance because of the large frozen magnetization and of the emergence spin wave modes coupling to resonance excitations. In this section we generalize the study in [3] to the case of equatorial states of ferromagnet with uniaxial anisotropy in an arbitrary direction, and a demagnetization field. In Section 4.1 we concentrate specifically on equatorial fixed points in the presence of spin wave excitations. In Section 4.2 we obtain the generalized Suhl's instability criterion. For this purpose, we consider first a general perturbation $\delta\hat{\psi}(\mathbf{r}, t)$ to the homogeneous steady field $\hat{\psi}_o$, in contrast to the spatially homogeneous perturbations of the previous section. The nature of instabilities are identified by linearizing equation (22) in $\delta\hat{\psi}$, around $\hat{\psi}_o$. Upon substituting $\hat{\psi} \equiv \hat{\psi}_o + \delta\hat{\psi}$ in equation (22), and confining to first order in $\delta\hat{\psi}$, we find,

$$i(1-i\alpha)\delta\dot{\hat{\psi}} = D\nabla^2\delta\hat{\psi} - (h_{a\parallel} - \omega + i\alpha\omega + \kappa\frac{1-|\hat{\psi}_o|^2}{1+|\hat{\psi}_o|^2})\delta\hat{\psi}$$ (39)

$$+2\kappa\Gamma\hat{\psi}_o(\hat{\psi}_o\delta\hat{\psi}^* + \hat{\psi}_o^*\delta\hat{\psi})$$

$$-h_{a\perp}\hat{\psi}_o\delta\hat{\psi} - \delta h_{m\parallel}\hat{\psi}_o$$

$$+\frac{1}{2}\delta H_m e^{-i\omega t} - \frac{1}{2}\hat{\psi}^2\delta H_m^* e^{i\omega t}.$$

11

Note that in the above equation (39), the dispersion term and the variations in the demagnetization field are nontrivial due to the perturbation being spatially inhomogeneous. Making now a spatial Fourier decomposition,

$$\delta\hat{\psi} = \sum_{\mathbf{q}} a_q(t)e^{i\mathbf{q}\cdot\mathbf{r}}; \quad \delta\psi^* = \sum_{\mathbf{q}} a^*_{-q}(t)e^{i\mathbf{q}\cdot\mathbf{r}}, \tag{40}$$

and substituting in equation (39) we obtain the mode equations for a_q with the propagation vector $\mathbf{q}$. Due to the Poisson bracket relations in equation (19), the mode amplitudes a_q also obey the Poisson bracket relation $\{a_q, a^*_{-q'}\} = i\delta_{q,q'}$.

The corresponding change in the demagnetization field is obtained using the relation

$$\nabla \cdot \delta\mathbf{H}_m = -4\pi\nabla \cdot \delta\mathbf{m}. \tag{41}$$

Here, $\delta\mathbf{m}$ is the change in the average local magnetization corresponding to $\delta\hat{\psi}$. This can be calculated using equation (13), and is given by

$$\delta\mathbf{m} = \Gamma\Big\{ (e^{-i\omega t} - \hat{\psi}_o^2 e^{i\omega t})\delta\psi^* + (e^{i\omega t} - \hat{\psi}_o^{*2} e^{-i\omega t})\delta\hat{\psi}, \tag{42}$$
$$i(e^{-i\omega t} + \hat{\psi}_o^2 e^{i\omega t})\delta\psi^* - i(e^{i\omega t} + \hat{\psi}_o^{*2} e^{-i\omega t})\delta\hat{\psi},$$
$$-2(\hat{\psi}_o\delta\psi^* + \hat{\psi}_o^*\delta\hat{\psi})\Big\}.$$

Using equation (40) in equation (42) we can write,

$$\delta\mathbf{m} = \sum_{\mathbf{q}} \mathbf{Z}_q(t)e^{i\mathbf{q}\cdot\mathbf{r}}, \tag{43}$$

where

$$\mathbf{Z}_q(t) = \Gamma\Big\{ a^*_{-q}(e^{-i\omega t} - \hat{\psi}_o^2 e^{i\omega t}) + a_q(e^{i\omega t} - \hat{\psi}_o^{*2} e^{-i\omega t}), \tag{44}$$
$$ia^*_{-q}(e^{-i\omega t} + \hat{\psi}_o^2 e^{i\omega t}) - ia_q(e^{i\omega t} + \hat{\psi}_o^{*2} e^{-i\omega t}),$$
$$-2(\hat{\psi}_o a^*_{-q} + \hat{\psi}_o^* a_q)\Big\}$$

$$= \mathbf{Z}^*_{-q}(t). \tag{45}$$

Consequently, it can be verified that

$$\delta\mathbf{H}_m = -4\pi\sum_{\mathbf{q}} \frac{\mathbf{q}}{q^2}(\mathbf{q} \cdot \mathbf{Z}_q)e^{i\mathbf{q}\cdot\mathbf{r}} \tag{46}$$

12

satisfies the constitutive relations in equation (6).

From equation (39), using equations (40) and (46), we have the mode equation satisfied by the amplitudes a_q,

$$i(1 - i\alpha)\dot{a}_q = \left[-Dq^2 - \left(h_{a\parallel} - \omega + i\alpha\omega + \kappa \frac{1 - |\hat{\psi}_o|^2}{1 + |\hat{\psi}_o|^2} \right) \right] a_q \tag{47}$$
$$+2\kappa\Gamma\hat{\psi}_o(\hat{\psi}_o a_{-q}^* + \hat{\psi}_o^* a_q)$$
$$-h_{a\perp}\hat{\psi}_o a_q - \delta h_{m\parallel}\hat{\psi}_o$$
$$+\frac{1}{2}\delta H_m e^{-i\omega t} - \frac{1}{2}\hat{\psi}_o^2 \delta H_m^* e^{i\omega t},$$

where δH_m and $\delta h_{m\parallel}$ are obtained from equation (46). If $\hat{\mathbf{q}}(\equiv \mathbf{q}/|\mathbf{q}|)$ is expressed in the spin frame as $\hat{\mathbf{q}} = \sin\theta_q(\cos\phi_q \hat{e}_1 + \sin\phi_q \hat{e}_2) + \cos\theta_q \hat{e}_\parallel$, then

$$\hat{\mathbf{q}} \cdot \mathbf{Z}_q = \Gamma\left[\sin\theta_q \left[a_q(e^{i(\omega t - \phi_q)} - \hat{\psi}_o^{*2} e^{-i(\omega t - \phi_q)}) \right. \right. \tag{48}$$
$$\left. +a_{-q}^*(e^{-i(\omega t - \phi_q)} - \hat{\psi}_o^2 e^{i(\omega t - \phi_q)}) \right]$$
$$\left. -2\cos\theta_q(\hat{\psi}_o a_{-q}^* + \hat{\psi}_o^* a_q) \right]$$

$$= \hat{\mathbf{q}} \cdot \mathbf{Z}_{-q}^*. \tag{49}$$

Here θ_q and ϕ_q are the polar and azimuthal angles made by the wave vector $\mathbf{q}$ in the spin frame spanned by $\hat{e}_1$, $\hat{e}_2$ and $\hat{e}_\parallel$. Substituting equation (48) in equation (46) and using the resultant expression for $\delta\mathbf{H}_m$ in equation (47), we can write

$$\dot{a}_q + iA_q a_q + iB_q a_{-q}^* = 0, \tag{50}$$

$$A_q = (1 - i\alpha)^{-1}\left[-Dq^2 - \left(h_\parallel - \omega + i\alpha\omega + \kappa \frac{1 - |\hat{\psi}_o|^2}{1 + |\hat{\psi}_o|^2} \right) \right. \tag{51}$$
$$+2\kappa\Gamma|\hat{\psi}_o|^2 - h_{a\perp}\hat{\psi}_o$$
$$\left. -2\pi\Gamma|2\hat{\psi}_o \cos\theta_q - \sin\theta_q(e^{-i(\omega t - \phi_q)} - \hat{\psi}_o^2 e^{i(\omega t - \phi_q)})|^2 \right]$$

$$B_q = (1 - i\alpha)^{-1}\left[2\kappa\Gamma\hat{\psi}_o^2 - 2\pi\Gamma\left(2\hat{\psi}_o \cos\theta_q \right. \right. \tag{52}$$
$$\left. \left. -\sin\theta_q(e^{-i(\omega t - \phi_q)} - \hat{\psi}_o^2 e^{i(\omega t - \phi_q)}) \right)^2 \right].$$

Similarly,

$$\dot{a}^*_{-q} - iA^*_{-q}a^*_{-q} + iB^*_{-q}a_q = 0. \tag{53}$$

Now we will analyze these mode equations (50) and (53) in some detail in the following subsections.

4.1   Stability of equatorial and related

fixed points As we noted in Section 3.1, the fixed points along the equator, P_1 and P_2, as well as the related fixed points P_3 and P_4 are possible when the pumping frequency ω coincides with the amplitude of the static parallel magnetic field $h_{a\|}$. The nature of stability of these fixed points can be studied by identifying a period map $\mathbf{M}$ using the mode equations (50) and (53). In this connection it must be remembered that the P-modes have inherent in them a time period $T = 2\pi/\omega$ arising from the frequency of the applied transverse field. Then the period map $\mathbf{M}$, defined through the equation,

$$\begin{pmatrix} a_q(T) \\ a^*_{-q}(T) \end{pmatrix} = \mathbf{M} \begin{pmatrix} a_q(0) \\ a^*_{-q}(0) \end{pmatrix}, \tag{54}$$

is obtained from equations (50) and (53) after integration through one period T. Numerically, the map $\mathbf{M}$ in equation (54) is obtained by evolving over a period T the two column vectors $(1,0)^T$ and $(0,1)^T$, taken as the initial vectors $(a_q(0), a^*_{-q}(0))^T$. The two columns so obtained then form the columns of the period map $\mathbf{M}$. From equations (30) and (31)-(33), there are effectively two tunable parameters, Ω and $b_\perp$ or ω and $h_{a\perp}$, that also fix the fixed point $\hat{\psi}_o$. If $\gamma_{q\pm}$ are the eigenvalues of the period map $\mathbf{M}$ for a given fixed point $\hat{\psi}_o$, the fixed point is unstable for a mode of wave vector $\mathbf{q}$ if $|\gamma_{q\pm}| > 1$. Figure 3 shows unstable regions in the $\cos\theta - \omega$ space as shaded regions for different values of the angle θ_q: (a) $\sin\theta_q = 0$, (b) $\sin\theta_q = 0.6$ and (c) $\sin\theta_q = 1$. Note that $\cos\theta$ here effectively stands for $h_{a\perp}$ through the relations (31)-(33). In Figure 4, the same regions are shown in the $h_{a\perp} - h_{a\|}$ plane. However, not all points on the plane are experimentally accessible if one requires a homogeneous background, due to the condition $0 \le h_{a\perp}^2 \le \kappa_{eff}^2 + \alpha^2\omega^2$. Note that θ_q defines the angle between the anisotropy axis and the plane of the ferromagnetic film. It should be emphasized that the global stability diagrams in Figures 3 and 4 are obtained under the condition that $\omega = h_{a\|}$. We find that the equatorial and related fixed points are always stable for the perpendicular field with its strength $h_{a\perp}$ less than the value determined by the pumping frequency, but become unstable when $h_{a\perp}$ is "decreased" below the generalized Suhl

14

threshold. There exists an interesting singular structure near the vicinity of $\omega = 0$ (Figure 3) or of $h_{a\parallel} = 0$ (Figure 4), which is very sensitive to the angle θ_q. These phase diagrams differ qualitatively from those for the conventional spin-wave instability near the ferromagnetic ground state.

4.2   Mode equations and Suhl's instability

It can be verified from equations (51) and (52) that $A_q = A_{-q}$ and $B_q = B_{-q}$, if we note $\hat{\mathbf{q}} \rightarrow -\hat{\mathbf{q}} \Rightarrow \theta_q \rightarrow \pi - \theta_q$ and $\phi_q \rightarrow \phi_q + \pi$. To begin with, we shall first suppress the oscillating terms with $exp[\pm i(\omega t - \phi_q)]$ and $exp[\pm 2i(\omega t - \phi_q)]$. Then, A_q and B_q in equation (50) are replaced by $\tilde{A}_q$ and $\tilde{B}_q$ given by

$$\tilde{A}_q = (1 - i\alpha)^{-1}\left[-Dq^2 - \left(h_\parallel - \omega + i\alpha\omega + \kappa\frac{1 - |\hat{\psi}_o|^2}{1 + |\hat{\psi}_o|^2}\right)\right. \tag{55}$$
$$+2\kappa\Gamma|\hat{\psi}_o|^2 - h_{a\perp}\hat{\psi}_o$$
$$\left. -2\pi\Gamma\left(4|\hat{\psi}_o|^2\cos^2\theta_q + \sin^2\theta_q(1 + |\hat{\psi}_o|^4)\right)\right]$$

$$\tilde{B}_q = (1 - i\alpha)^{-1}\left[2\kappa\Gamma\hat{\psi}_o^2 - 2\pi\Gamma\left(4\hat{\psi}_o^2\cos^2\theta_q - 2\sin^2\theta_q\hat{\psi}_o^2\right)\right] \tag{56}$$

Then equation (47) can be written in terms of normal modes, after a Bogoliubov type linear transformation $a_q = \lambda_q b_q - \mu_q b^*_{-q}$, to a new variable b_q. Here, on account of both a_q and b_q obeying Poisson bracket relations, λ_q and μ_q satisfy the condition,

$$\lambda_q\lambda_{-q} - \mu_q\mu^*_{-q} = 1. \tag{57}$$

However, $\lambda_q = \lambda_{-q}$ and $\mu_q = \mu_{-q}$, as will be shown below. With this change, using equation (57), equation (50) becomes

$$\dot{b}_q + i\left[\lambda_q(\lambda_q\tilde{A}_q - \mu^*_q\tilde{B}_q) + \mu_q(\mu^*_q\tilde{A}^*_q - \lambda_q\tilde{B}^*_q)\right]b_q + i\left[\lambda_q(\lambda_q\tilde{B}_q - \mu_q\tilde{A}_q)\right. \tag{58}$$
$$\left. +\mu_q(\mu_q\tilde{B}^*_q - \lambda_q\tilde{A}^*_q)\right]b^*_{-q} = 0.$$

In order for b_q to represent normal modes, the last term in equation (58) must vanish. This condition along with equation (57) determines λ_q and μ_q. After some straight forward algebra we find

$$\lambda_q = \cosh\frac{\xi_q}{2}; \quad \mu_q = \sinh\frac{\xi_q}{2}e^{i\nu_q}, \tag{59}$$

$$\tanh \xi_q = \frac{2|\tilde{B}_q|}{\tilde{A}_q + \tilde{A}_q^*}; \qquad e^{2i\nu_q} = \frac{\tilde{B}_q}{\tilde{B}_q^*}. \tag{60}$$

Since $\tilde{A}_q = \tilde{A}_{-q}$ and $\tilde{B}_q = \tilde{B}_{-q}$ from equations (55) and (56), it follows that $\lambda_q = \lambda_{-q}$ and $\mu_q = \mu_{-q}$. Substituting for λ_q and μ_q from equations (59) and (60) in equation (58) gives,

$$\dot{b}_q + i(\omega_q - i\eta_q)b_q = 0, \tag{61}$$

$$\omega_q^2 = \frac{1}{2}[(\tilde{A}_q + \tilde{A}_q^*)^2 - 4|\tilde{B}_q|^2]; \tag{62}$$

$$\eta_q = \frac{i}{2}(\tilde{A}_q - \tilde{A}_q^*), \tag{63}$$

with solutions

$$b_q \propto e^{-i\omega_q t - \eta_q t}. \tag{64}$$

In equation (64), ω_q is the eigen frequency for the spin-wave normal mode and η_q is its damping constant.

Next we analyze the spin wave dynamics in the presence of oscillating terms in equation (50). We notice from equations (51) and (52) that terms with $\exp[\pm i\omega t]$ and $\exp[\pm 2i\omega t]$ appear in equation (50). First, we suppress all other oscillating terms retaining only the term with $\exp[-2i\omega t]$. The equation (61) is modified to

$$\dot{b}_q + i(\omega_q - i\eta_q)b_q + ie^{-2i\omega t}\rho b_{-q}^* = 0, \tag{65}$$

where

$$\rho = \lambda_q(\lambda_q \tilde{B}_q^{1\prime\prime} - \mu_q \tilde{A}_q^{\prime\prime}) + \mu_q(\mu_q \tilde{B}_q^{2\prime\prime} - \lambda_q \tilde{A}_q^{\prime\prime*}), \tag{66}$$

$$\tilde{A}_q^{\prime\prime} \equiv \frac{2\pi\Gamma}{1 - i\alpha} \sin^2 \theta_q \hat{\psi}_o^2. \tag{67}$$

$$\tilde{B}_q^{1\prime\prime} \equiv \frac{-2\pi\Gamma}{1 - i\alpha} \sin^2 \theta_q \hat{\psi}_o^4, \tag{68}$$

$$\tilde{B}_q^{2\prime\prime} \equiv \frac{-2\pi\Gamma}{1 + i\alpha} \sin^2 \theta_q. \tag{69}$$

If we assume solutions of the form $b_q = b_q^o(t)e^{-i\omega t - \eta_q}$, equation (65) can be written as

$$\dot{b}_q^o + i(\omega_q - \omega)b_q^o + \rho b_{-q}^{o*} = 0, \tag{70}$$

or, taking a second derivative in time, and using its complex conjugate,

$$\left[\partial_t^2 + (\omega_q - \omega)^2 - |\rho|^2\right]b_q^o = 0. \tag{71}$$

The necessary condition to see a growth of spin waves against P-mode is then given by

$$(\omega_q - \omega)^2 - |\rho|^2 \leq 0. \tag{72}$$

When this condition is satisfied, the normal mode grows as

$$b_q \propto \exp\left[(|\rho|^2 - (\omega_q - \omega)^2)^{1/2}t\right]\ \exp[-i\omega_q t - \eta_q t]. \tag{73}$$

Thus, to see an exponential catastrophic growth of b_q, we should have

$$(\omega_q - \omega)^2 + \eta_q^2 \leq |\rho|^2. \tag{74}$$

With a similar argument for the term $e^{-i\omega t}$, repeating equations (65) - (74) we obtain a condition analogous to equation (74),

$$(\omega_q - \frac{\omega}{2})^2 + \eta_q^2 \leq |\tilde{\rho}|^2, \tag{75}$$

with

$$\tilde{\rho} = \lambda_q(\lambda_q \tilde{B}_q^{1\prime} - \mu_q \tilde{A}_q{}') + \mu_q(\mu_q \tilde{B}_q^{2\prime} - \lambda_q \tilde{A}_q^{\prime*}), \tag{76}$$

$$\tilde{A}_q{}' \equiv \frac{-2\pi\Gamma}{1 - i\alpha}2\sin\theta_q\cos\theta_q(|\hat{\psi}_o|^2 - 1)\hat{\psi}_o, \tag{77}$$

$$\tilde{B}_q^{1\prime} \equiv \frac{-2\pi\Gamma}{1 - i\alpha}4\sin\theta_q\cos\theta_q\hat{\psi}_o^3, \tag{78}$$

$$\tilde{B}_q^{2\prime} \equiv \frac{2\pi\Gamma}{1 + i\alpha}4\sin\theta_q\cos\theta_q\hat{\psi}_o^*. \tag{79}$$

In the above analysis, the angle θ_q - the angle between the anisotropy axis and the $x-y$ plane plays a crucial role. From equations (51) and (52), we note that

when $\theta_q = \pi/2$, terms with $exp[\pm i\omega t]$ vanish. Consequently, the resonance at $\omega/2$ is absent. When $\theta_q = 0$, the anisotropy axis is in the $x-y$ plane, and both the resonances ($\omega_q = \omega/2, \omega$) vanish. Equations (74) with equations (66)-(69), and equation (75) with equations (76)-(79) provide new criteria for spin-wave instabilities of P-modes. The global stability diagrams depicted on the basis of this new criteria are given in Figure 5, which nicely characterize the principal part of the boundary curves between stable and unstable regions in Figure 3 and 4. In particular, consistent with Figures 3 and 4 obtained from the period map, there is a singular structure near the vicinity of $\omega = 0$ (Figure 5(b'), 5(c')) or of $h_{a\parallel} = 0$ (Figure 5(b") and 5(c")) sensitive to the angle θ_q.

5   Conclusion

We have investigated non-equilibrium states of nanoscale ferromagnets with uniaxial anisotropy, in the presence of an oscillating field transverse to the axis of anisotropy. The saturation magnetization can be driven even to the equatorial plane perpendicular to the anisotropy axis. The P-modes correspond to new non-equilibrium states lying far from the anisotropy axis. The stability of the P-modes under uniform and spin wave perturbations has been studied in general.

Specifically we have identified new equatorial and other fixed points, which exhibit a more complex dynamical phenomena. These novel states (fixed points) are realized in the case that the pumping frequency coincides with the amplitude of the static parallel field. We concentrated on the spin-wave instability of the above states and found that these states are always stable for the perpendicular field with its strength $h_{a\perp}$ less than the value determined by the pumping frequency, but become unstable when $h_{a\perp}$ is "decreased" below the generalized Suhl threshold. By using the period map the global stability diagram in $h_{a\perp} - h_{a\parallel}$ plane is obtained, which shows an interesting singular structure which is very sensitive to the angle θ_q between the spin-wave propagation vector (the film plane) and the direction of the uniaxial anisotropy.

Closely following the original paper by Suhl based on Bogoliubov-type transformation, we have also obtained the generalized Suhl instability condition in a form of coupled spin-wave equations, which recovers the major part of the global phase diagram obtained by the period map. It should be noticed that resonance occurs at the frequencies $\omega_q = \omega/2$ and $\omega_q = \omega$ for $\theta_q \neq 0$, but is absent for $\theta_q = 0$, i.e., when the axis of uniaxial anisotropy lies in the plane of the ferromagnet. The present findings differ qualitatively from those for the conventional Suhl instability near the ground state of uniaxial ferromagnets. Various nonlinear dynamics aspects including spin wave turbulence (see for example ref. [22,23]) beyond the generalized Suhl instability will constitute

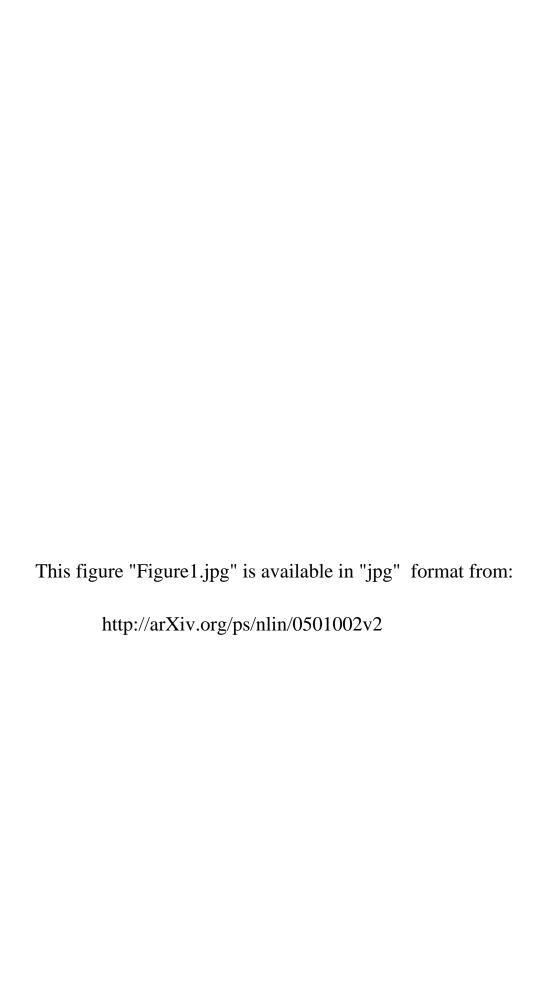subjects which we intend to study in future.

Acknowledgements

References

[1] R. W. Damon, Rev. Mod. Phys. 25 (1953) 239.

[2] N. Bloembergen and S Wang, Phys. Rev. 93 (1954) 72.

[3] H. J. Suhl, J. Phys. Chem. Solids 1 (1967) 209.

[4] B. Hillerbands and K. Ounadjela, Spin Dynamics in Confined Magnetic Structures (Vol. I and II), Springer-Verlag, Berlin, 2002.

[5] S. M. Rezende, Phys. Rev. Lett. 56 (1986) 1070.

[6] P. Bryant, C. Jeffries and K Nakamura, Phys. Rev. Lett. 60 (1988) 1185.

[7] P. Bryant, C. Jeffries, and K. Nakamura, Phys. Rev. A 38 (1988) 4223

[8] T. L. Carroll, M. L. Pecora and F. J. Rachford, J. Appl. Phys. 64 (1988) 5396.

[9] V. S. L' vov, Wave Turbulence under Parametric Excitation, Springer-Verlag, Berlin, 1994.

[10] P. E. Wigen (ed.), Nonlinear Phenomena and Chaos in Magnetic Materials, World Scientific, New Jersey, 1994.

[11] J. Becker, F. Rödelsperger, Th. Weyrauch, H. Benner, W. Just and C. Cenys, Phys. Rev. E 59 (1999) 1622.

[12] I. Laulicht and P. E. Wigen, J. Magn. Magn. Mater. 207 (1999) 103.

[13] M. Lakshmanan and M. Daniel, Physica A 107 (1981) 533.

[14] A. M. Kosevich, B. A. Ivanov and A. S. Kovalev, Phys. Rep. 194 (1990) 117.

[15] H. J. Mikeska and M. Steiner, Adv. Phys. 40 (1990) 191.

[16] P. Podio-Guidugli and G. Tomassetti, SIAM J. Appl. Maths 64 (2004) 1887.

[17] F. G. Mertens and A. R. Bishop in "Lecture Notes in Physics: Nonlinear Science at the Dawn of the 21st Century", P. L. Christiansen, M. P. Sorensen and A. C. Scott, eds. Springer, Berlin 2000.

[18] G. Bertotti, I. D. Mayergoyz and C. Serpico, Phys. Rev. Lett. 87 (2001) 217203.

[19] G. Bertotti, I. D. Mayergoyz and C. Serpico, Phys. Rev. Lett. 86 (2001) 724.

[20] L. Landau and E. Lifshitz, Physik. Zeitsch. d. Sowjetunion 8 (1935) 153.

[21] M. Lakshmanan and K. Nakamura, Phys. Rev. Lett. 53 (1984) 2497.

[22] A. R. Bishop, L. J. Campbell and P. J. Channell (eds.), Fronts, Interfaces and Patterns, North-Holland, Amsterdam, 1984.

[23] M. C. Cross and P. C. Hohenberg, Rev. Mod. Phys. 65 (1993) 851.

Fig. 1. Stereographic projection from the unit sphere onto a complex plane. Any point $\hat{\mathbf{m}}$ on the surface of the sphere can be mapped onto a point ψ on the complex plane as shown above. Points on the upper hemisphere are mapped onto points inside the unit circle, while points on the lower hemisphere are mapped to the points outside the unit circle. All points at ∞ in the complex plane are identified with the south pole $\mathbf{S}$.

Fig. 2. Phase portrait obtained using equation (22), assuming spatial homogeneity of $\hat{\psi}$, for the choice $h_{a\parallel} = \omega$, $\kappa_{eff} = 0.1$, $D = 1$, $\alpha = 0.01$ and $\omega = 0.8$. The initial value of $\mathrm{Im}\hat{\psi}$ is fixed at 0.5, while $\mathrm{Re}\hat{\psi}$ is varied from -3 to 5. (a) $b_{a\perp}^2 = 1 + \Omega^2$, with fixed points corresponding to $|\hat{\psi}_o|^2 = 1, P_1 = (-0.99, 0.12)$ (unstable fixed point), and $P_2 = (0.99, -0.12)$ (stable fixed point). (b) $b_{a\perp}^2 = (1 + \Omega^2)/2$, with fixed points at $(-.99, .12)$ (unstable fixed point), $(0.41, -0.03)$ (stable fixed point), $(0.99, -0.12)$ (saddle), $(2.4, -0.2)$ (stable fixed point). (c) Enlarged image of the central portion in (b) showing the two fixed points, one stable, and another a saddle. In (b) and (c), the fixed points P_1, etc., may be identified near the respective numerical values.

Fig. 3. Unstable regions in the $(\cos\theta, \omega)$ space shown by dark regions, as obtained from the period map $\mathbf{M}$. Here, $\alpha = 0.01$, $\kappa_{eff} = 0.1$, $q = 0.1$. $(a)\ \sin\theta_q = 0$, $(b)\sin\theta_q = 0.6, (c)\sin\theta_q = 1$.

Fig. 4. Unstable regions corresponding to Figure 3 in the $(h_{a\parallel}, h_{a\perp})$ space shown by dark regions, as obtained from the period map $\mathbf{M}$. Here, $\alpha = 0.01$, $\kappa_{eff} = 0.1$, $q = 0.1$. $(a)\ \sin\theta_q = 0$, $(b)\sin\theta_q = 0.6, (c)\sin\theta_q = 1$. Not all points in the plane are accessible if one requires a homogeneous background, due to the condition $0 \le h_{a\perp}^2 \le \kappa_{eff}^2 + \alpha^2\omega^2$.

Fig. 5. Unstable regions in the $(\cos\theta, \omega)$ plane (left) and the corresponding regions in the $(h_{a\parallel}, h_{a\perp})$ plane (right). The parameter values correspond to the values for (b) and (c) in Figures 3 and 4. Instabilities at $\omega_q = \omega$ are indicated by dots $(\cdot)$, and those at $\omega_q = \omega/2$ by plus $(+)$. For $\sin\theta_q = 0$, both ρ and $\tilde{\rho}$ vanish as seen from equations $(66) - (69)$ and $(76) - (79)$, and hence no instability occurs. For $\sin\theta_q = 1$, the instability at $\omega_q = \omega/2$ does not occur since $\tilde{\rho}$ vanishes as seen from equations $(76) - (79)$.

This figure "Figure1.jpg" is available in "jpg" format from:

http://arXiv.org/ps/nlin/0501002v2

This figure "Figure2.jpg" is available in "jpg" format from:

http://arXiv.org/ps/nlin/0501002v2

This figure "Figure3.jpg" is available in "jpg" format from:

http://arXiv.org/ps/nlin/0501002v2

This figure "Figure4.jpg" is available in "jpg" format from:

http://arXiv.org/ps/nlin/0501002v2

This figure "Figure5.jpg" is available in "jpg" format from:

http://arXiv.org/ps/nlin/0501002v2